

Model of space- and energy-dependent electron flux density

A. V. Vasenkov

Institute of Thermophysics and Novosibirsk State University, Novosibirsk 630090, Russia

(Received 13 January 1999)

Analytic representation for the space- and energy-dependent electron flux density in terms of a phenomenological model was developed. The model was applied to electron energy degradation in gaseous argon. Flux density data were also generated from Monte Carlo simulations for 0.3–3.0 keV incident electrons. These data were used to determine adjustable parameters in our phenomenological model. From the nature of the cross section input to this model, we expect that the scaled flux density for most atomic and molecular gases will be similar to that obtained in this study. [S1063-651X(99)51605-X]

PACS number(s): 52.25.-b, 41.75.Fr, 52.65.-y, 87.50.Gi

Ionization sources, such as beams of x rays and high-energy beams of neutral or charged particles, interact with a gas by generating fast electrons. The energy from the ionization source is transmitted to the gas atoms and molecules by these energetic electrons. Therefore, the activity of the ionization source can be simulated by the activity of a high-energy electron beam. An electron beam, while passing through a gas, induces both ionization and excitation of various degrees of freedom of gas molecules or atoms. Both the electron distribution and properties of gaseous mediums are changed as this occurs. Characteristics of electron beam–gas interaction can be expressed in terms of the electron flux as a function of energy and position. This electron flux contains the basic information about the radiation field of electrons in a gas. Interest in modeling the electron flux occurs in radiation chemistry and biology, radiological physics, plasma sciences, atmospheric physics, astrophysics, plasma processing in the microelectronics industry, and plasma cleaning of flue gases. Kinetic theory, which involves direct solutions of the Boltzmann equation, can give a comprehensive description of the electron flux. A rich variety of numerical solutions of the Boltzmann equation has been reported [1]. While these solutions provide clear insight into the physics of electron energy distribution formation, they are not applicable to problems involving spatial aspects of electron degradation. Simplified solutions like these are often necessary due to the mathematical difficulties encountered in direct solutions of the Boltzmann equation with spatial dependence. Green and Singhal [2] developed an analytic representation for the spatial yield spectra in terms of a model containing three simple microplumes. Using this model, a yield for any inelastic state at any position in the medium can be approximately calculated. This present study is directed towards correlating the structural properties of cross sections with the space- and energy-dependent flux density in an attempt to establish general principals of spatial variations of electron degradation in gases.

For numerous cases of electron scattering and transport in a gas the appropriate geometry is one spatial dimension. For this geometry the steady state transport equation for electrons is

$$\begin{aligned} \cos(\theta) \frac{\partial}{\partial Z} \Phi(Z, E, E_p, \vec{k}) + n_g \Sigma(E) \Phi(Z, E, E_p, \vec{k}) \\ = S(Z, E, E_p, \vec{k}) + n_g \int \Sigma(E' \rightarrow E, \vec{k}' \rightarrow \vec{k}) \\ \times \Phi(Z, E', E_p, \vec{k}') d\Omega' dE', \end{aligned} \quad (1)$$

where Φ is the triple differential [with respect to the distance (Z) from the injection point, current energy (E), and directions (\vec{k})] flux density, E_p is the incident electron energy, S is the source of electrons, $\Sigma(E)$ and $\Sigma(E' \rightarrow E, \vec{k}' \rightarrow \vec{k})$ are the total and differential cross sections summed over all scattering processes, and n_g is the gas density. The integrations on the right-hand side of Eq. (1) are over the initial solid angle Ω' and energy E' . For the majority of practically important cases the double differential flux density $\Phi(Z, E, E_p)$ (i.e., the triple differential flux density integrated over all directions \vec{k}) is of interest. A normalization for the double differential flux density is chosen in the form $\int \Phi(Z, E, E_p) \sigma_i(E) dE dZ = 1$, where σ_i is the ionization cross section. This property of flux density is useful for calculations of the efficiency for production of any electron state of atoms or molecules and, consequently, initial plasma composition [3]. (By the term “initial plasma composition” we mean the composition of plasma that is formed immediately following electron collisions and degradation.)

We start the construction of analytical representation for $\Phi(Z, E, E_p)$ from an investigation of flux density characteristics. With this aim in mind, it is useful to separate electrons into two categories: low-energy [$E < E^*(E_p)$] and high-energy [$E \geq E^*(E_p)$] electrons. Then, the electron flux density is equal to the sum of the low-energy (Φ^I) and high-energy (Φ^{II}) flux densities. Recently, taking argon as an example, it was shown that the low-energy part of the flux density may be approximately expressed by multiplication of the space-dependent with energy-dependent terms [3]:

$$\Phi^I(z, E, E_p) = \Psi(z, E_p) g(E, E_p), \quad (2)$$

where $\Psi(z, E_p)$ is equal to $[a_0(E_p)]^{-1} \exp\{a_1(E_p)z - a_2(E_p)[z + a_3(E_p)]^2\}$, $z = Z/R_0$ (R_0 is range), the values for

the parameters are given in [3]. Considering Eq. (1) and Eq. (2), one can easily obtain a transport equation for the determination of $g(E, E_p)$. The electron source in this equation is ionization induced by high-energy electrons. It should be noted that the energy distribution of secondary electrons produced by this source is nearly independent of the incident energy for sufficiently high E_p . This is because of the properties of differential ionization cross sections. On the other hand, inelastic cross sections are power dependent on energy in the low-energy range. Thus, $g(E, E_p)$ can be represented by $\sum_i A_i(E_p) E^{-|\alpha_i(E_p)|}$. One should expect parameters A_i and α_i to be independent of E_p for sufficiently high incident energies.

The properties of Φ^{II} are more complex than those of Φ^I . In particular, the high-energy part of the flux density cannot be separated into the space-dependent and energy-dependent terms. In the construction of the analytical representation for Φ^{II} we started from an investigation of properties of the high-energy part of the flux density, integrated over the distance [$\Phi^{II}(E, E_p)$]. The latter flux density is inversely related to the energy loss function $L(E, E_p)$ [4]. In the approach of the continuous slowing down approximation, $L(E, E_p)$ varies in exactly the same manner as do inelastic cross sections. The cross sections of various inelastic collisions in the high-energy range achieve asymptotic agreement with the results of the Born-Bethe approximation. Consequently, at $E^*(E_p) < E < E_p$, the analytical representation for the reciprocal of flux density is to be looked for as $\ln(E/I^*)/E^\beta$, where I^* is energy spent by high-energy electrons, on the average, for a collision, and β is a parameter. A special approach should be developed to obtain analytical representation for flux density at energies close to the incident energy. At these energies electrons spent the energy mainly to produce ionization. In the limit $E \gg I_i$ (where I_i is the ionization potential) the differential ionization cross section approaches the Mott cross section. The Mott cross section structure suggests looking for the analytical representation for the reciprocal of the flux density in the form $(E_p - E)^{-\eta}$, where η is a parameter. When one considers the spatial structure of the flux density, elastic collisions should be included. We suggest that the analytical representation for $\Phi^{II}(z, E, E_p)$ can be built from an analytical representation for the energy-dependent flux density with parameters dependent on the distance from the injection point.

The proposed approach was applied to electron energy degradation in gaseous argon. Argon has been selected because a representative basic set of detailed cross sections was available and the number of electronic states was moderate. In the first stage, we obtained the space- and energy-dependent flux density. This flux density was calculated using a Monte Carlo method of electron energy degradation and electron scattering. Energy degradation was simulated assuming that after excitation an atom would be found in a composite optically forbidden state, or in the optically allowed $4s_{3/2}$, $4s'_{1/2}$, $3d_{3/2}$, $3d'_{3/2}$, and composite optically allowed states. The M -shell ionization (with threshold $I_M = 15.76$ eV) event and the L -shell ionization (with threshold $I_L = 250.42$ eV) event were considered as well. During an L -shell ionization event an Auger electron (with kinetic energy $E_A = 218.9$ eV) was assumed to be emitted with 100% efficiency. Cross sections for the above-mentioned processes

were calculated using the formulas given in [3,5]. Elastic [3] and inelastic [6] scattering of an electron by argon atoms were also considered. The details of our Monte Carlo approach have been reported in [3].

In the next stage, we fitted [$\Phi^{II}(z, E, E_p)$] $^{-1}$ to Monte Carlo data. After a few attempts we found better fits to the results of direct simulation by letting

$$\begin{aligned} \Phi^{II}(z, E, E_p)^{-1} \Psi(z, E_p) &= \Lambda(E_p) [1 + \psi(z) \delta(E - E_A)] \\ &\times \left\{ \frac{\ln[C(z)E/E_p + H(\epsilon(E_p) - E)]}{2} \right. \\ &\left. + \exp(\varphi(z)) \left[\frac{E_p - E - \Gamma(z, E_p)}{E_p} \right]^{-\eta(z)} H(z) \right\}, \quad (3) \end{aligned}$$

where $\psi(z)$, $\Xi_l(z)$, $\beta_l(z)$, $\varphi(z)$, $\eta(z)$, and $C(z)$ are represented by polynomials in z and $\Lambda(E_p)$ is represented by a polynomial in E_p [6], $\epsilon(E_p) = 0.2/(1 + 10^{-2}E_p^{-10})$, and current and incident energies are in units of 1 keV. $\Gamma(z, E_p) = \xi E_p + \Delta(z) E_p^2$ [$\Delta(z)$ is a polynomial in z] is included in Eq. (3) to account for the decrease in energy of primary electrons with the increase in distance from the injection point. By primary electrons I mean incident electrons that scattered or degraded in energy. H is a unit step function equal to 0 at an argument of function less than or equal to 0. The results of fitting Eq. (3) to Monte Carlo data are shown in Figs. 1(a) and 1(b) for two incident energies and three longitudinal values. The contribution of the second term (in the braces) on the right-hand side of Eq. (3) is shown in Figs. 1(a) and 1(b) by dashed lines. This term represents the flux density at energies close to the incident energy. Including a unit step function in this term reflects the fact that the high-energy part of the flux density at $z=0$ is formed mainly by contribution from the source. The first term (in the braces) represents the flux density at lower energies. (The contribution of this term is shown in the figures as solid lines.) Including unit step functions (with $\bar{z}_0 = 1.0$, $\bar{z}_1 = 0.70$, $\bar{z}_2 = 0.25$) in the first term reflects the drastic changes of flux density with distance from the injection point. Figures 1(a) and 1(b) show that with the increase in distance the energy spectrum of the flux density has few high-energy electrons. This is because of the energy degradation and scattering of the electron beam. The contribution of Auger electrons to flux density is represented by including the Dirac delta function on the right-hand side of the equation. Comparison with the Auger electron contribution, generated from the Monte Carlo simulation and obtained using Eq. (3), is shown on an enlarged scale in the upper inset of Fig. 1(b). At $E_p = 0.3$ keV the contribution of Auger electrons, as shown in Fig. 1(a), is insignificant.

We might note that our fits are not of uniform quality over the entire range of distances and incident energies. Thus, the fits are poorer at lower incident energies, especially at a distance from the injection point. This is because first, in the low-energy range, inelastic cross sections do not follow the Born-Bethe approximation and each of them has its indi-

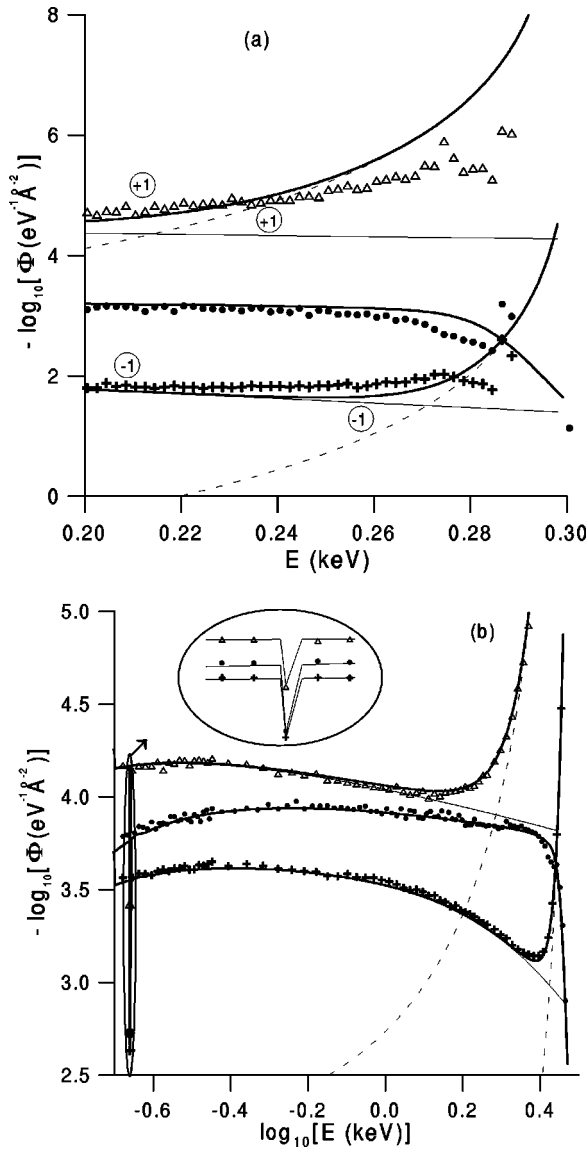


FIG. 1. Reciprocal of electron flux vs current energy at two incident energies and three distances from the injection point: (a) $E_p = 0.3$ keV, $R_0 = 1.88 \cdot 10^{-6}$ g/cm²; (b) $E_p = 3.0$ keV, $R_0 = 49.28 \cdot 10^{-6}$ g/cm². The Monte Carlo calculations are represented by the following symbols: ●, $z = 0$; +, $z = 0.448$; △, $z = 0.933$; and the analytic fit using Eq. (3) is represented by the following lines: solid line, contribution from the first term; dashed line, contribution from the second term; thick solid line, total contribution.

vidual dependence on energy, and second, the differential elastic cross section structure is rather complex.

In the final stage we find that it is convenient to represent the flux density for $E < E_A - W^*$ by

$$\Phi(z, E, E_p) = \Psi(z, E_p) g(E, E_p) + \Phi^{II}(z, E, E_p), \quad (4)$$

where $g(E, E_p)$ is determined by the following equation:

$$g(E, E_p) = \sum_{i=0}^1 A_i(E_p) E^{-|\alpha_i(E_p)|} H(E_A - W^* - E).$$

Here W^* is the first excitation potential of argon; $A_i(E_p)$ and $\alpha_i(E_p)$ ($i = 0, 1$) are represented by polynomials [6].

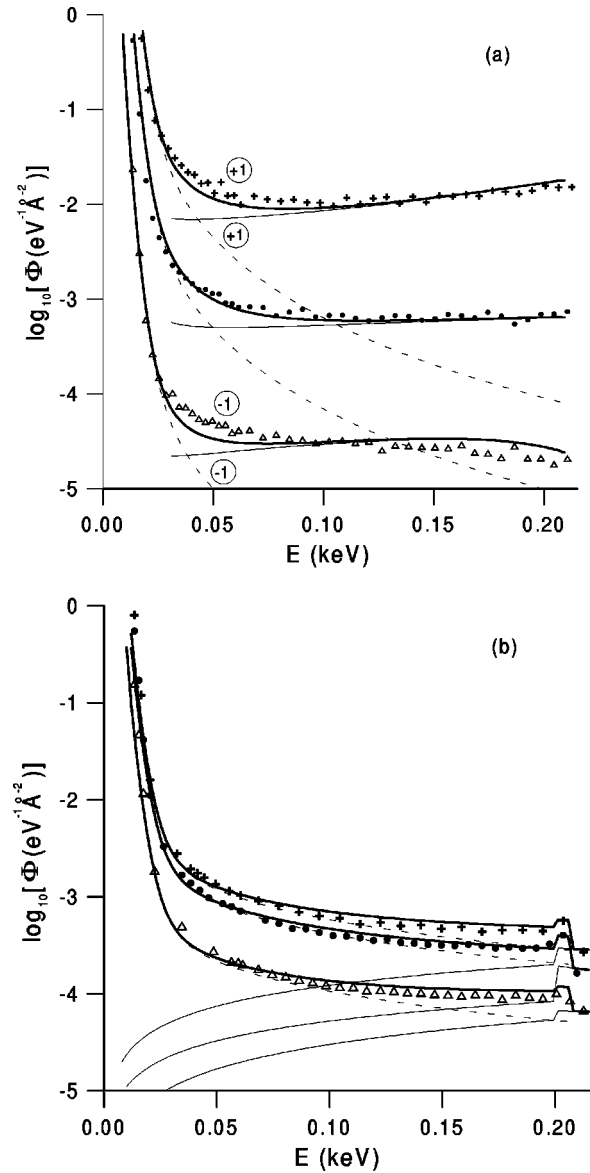


FIG. 2. Low-energy part of electron flux calculated by the Monte Carlo method is compared with the analytic fit using Eq. (4): dashed line, contribution from the first term; solid line, contribution from the second term; thick solid line, total contribution. Conditions and other designations are the same as in Fig. 1.

A comparison is given in Figs. 2(a) and 2(b) between $\Phi(z, E, E_p)$ obtained using Eq. (4) and the low-energy part of the flux density calculated by the Monte Carlo method. The analytical formula and Monte Carlo data are in agreement throughout the entire energy range considered. For $E_p = 0.3$ keV, the first term on the right-hand side of Eq. (4) contributes significantly only at energies close to excitation potentials of argon. In the case of $E_p = 3.0$ keV, the contribution from the first term is controlling or significant for the entire energy range shown in Fig. 2(b).

In summary, a phenomenological model for the space- and energy-dependent electron flux density was developed. Using this model, flux density was represented on the basis of balance between three terms, by the convention that represents low-energy, middle-energy, and high-energy parts of the flux density. In doing so, we converted exceedingly complex quantities into simple components. The model was ap-

plied to electron energy degradation in gaseous argon but we expect that this model can be used for other gases. This hypothesis is inspired by the nature of electron-atom and electron-molecule cross sections [2]. The inelastic cross sections differ markedly from species to species, but the individual inelastic cross sections divided by the total inelastic cross section are fairly similar from species to species. When one considers the spatial variations of electron degradation, one must include the total elastic and elastic differential cross sections. The total and differential elastic cross sections vary greatly in magnitude from species to species, but the ratio of these cross sections is fairly similar from one species

to another within the energy range of interest. Thus, we expect that the scaled flux density for most atomic and molecular gases will be similar to that obtained in this study. The scaled factor will be a function of the number of electrons per atom (or molecule) and the atomic (or molecular) weight of substance.

This research was supported in part by the Russian Foundation for Basic Research under Grant No. 99-03-32452a, and in part by the Russian State Program for Support of the Integration of Education and Science under Contract No. 274.

-
- [1] M. Kimura, M. Inokuti, and M. A. Dillon, in *Advances in Chemical Physics*, edited by I. Prigogine and S. A. Rice (Wiley, New York, 1993), Vol. 84, p. 193.
- [2] A. E. S. Green and R. P. Singhal, *Geophys. Res. Lett.* **6**, 625 (1979).
- [3] A. V. Vasenkov, *Phys. Rev. E* **57**, 2212 (1998).
- [4] V. P. Konovalov and E. E. Son, in *Khimiya Plazmy*, edited by B. M. Smirnov (Energoatomizdat, Moscow, 1987), Vol. 14, p. 194.
- [5] E. Eggarter and M. Inokuti, Argonne National Laboratory Radiological and Environmental Research Division Report No. ANL-80-58, 1980, p. 29.
- [6] A. V. Vasenkov (unpublished).